

Transient Nucleation near the Mean-Field Spinodal

A. O. Schweiger* and W. Klein

Center for Computational Science and Department of Physics, Boston University, Boston, MA, 02215

Nucleation is considered in a one-dimensional ϕ^4 model with a non-conserved order parameter and long-range interactions. For a sufficiently large system with a slow relaxation to metastable equilibrium, there is a non-negligible probability of nucleation occurring before reaching metastable equilibrium. This process is referred to as transient nucleation. The critical droplet is defined to be the object of maximum likelihood that nucleates the system with probability 1/2. Time-dependent droplet profiles and nucleation rates are derived; theoretical results are compared to computer simulation. The analysis reveals a distribution of nucleation times with a distinct peak characteristic of a non-stationary nucleation rate. Under the quench conditions employed, early-time critical droplets are more compact than the droplets found in metastable equilibrium simulations and theoretical predictions.

PACS numbers: 05.70.Ln; 64.60.Qb; 82.20.Db

I. INTRODUCTION

Standard nucleation theory predicts a single metastable equilibrium nucleation rate, which gives rise to an exponential distribution of nucleation times. However, a key assumption in the application of the standard theory is that the system relaxes into metastable equilibrium. During this relaxation, the system has a finite probability of decaying to the stable phase via an isolated droplet. We will refer to this as transient nucleation. This process is of both practical and theoretical interest. Experimentally, transient nucleation has been observed in the laser melting of thin silicon films [1], crystallization in amorphous alloys [2, 3], and liquid crystals [4]. Theoretical work has concentrated on mean-field kinetic descriptions [5, 6, 7, 8, 9, 10]. Studies of transient nucleation in ϕ^4 models [11, 12, 13] have shown a distribution of nucleation times with a distinct peak and exponential tail.

Our objective is to study transient nucleation rates and transient critical-droplet profiles in systems with long-range interactions near the (pseudo) spinodal [14, 17].

To make these ideas precise, we consider purely dissipative dynamics described by a Markovian Langevin equation that is a sum of a deterministic drift term and a stochastic term with zero mean. For this paper, we define the metastable well to be the set of configurations that would follow the (noiseless) deterministic drift to a stationary point other than the global energy minimum. The metastable well boundary \mathfrak{B} consists of configurations that, upon perturbation, would each drift to the metastable minimum with probability 1/2. A similar definition is employed by Roy et al. [15]. Transient critical droplets are characterized by the most probable configuration on the metastable well boundary at a given time t since the quench.

Experimentally, we define the *nucleation time* as the

latest time since the quench that the system was located on the metastable well boundary; the *nucleating droplet* is the corresponding system configuration. A system has nucleated when there is a negligible probability of returning to the metastable well.

Because the nucleation rate is an extensive quantity, transience is best observed when the relaxation to metastable equilibrium is slow and the system size is large. Our study examines transient nucleation near the spinodal, where the relaxation time is dominated by critical slowing down. Our primary results are that in magnetic field quenches at a temperature below the critical temperature the nucleation rate is adequately described by a quasi-equilibrium theory and that the droplets are more compact than those that nucleate near the spinodal in metastable equilibrium.

In Sec. II, we introduce the model and review the field theoretic treatment of nucleation near the mean-field spinodal, the basis for the subsequent analysis. Section III considers the time-dependent likelihood of non-equilibrium states during relaxation to metastable equilibrium. In Sec. IV, we find the time-dependent nucleation rate and transient critical droplet as a perturbation about the metastable equilibrium critical droplet. In Sec. V, we compare our theoretical treatment to results from computer simulation. Section VI interprets and compares our results to previous work.

II. METASTABILITY NEAR THE MEAN-FIELD SPINODAL

We consider a one-dimensional ferromagnetic system with long-range interactions prepared in equilibrium with an external field initially in the negative- z direction. At time $t = 0$, the field is set in the positive- z direction and the system then evolves into metastable equilibrium; it will ultimately escape via nucleation. The system will have an ordered ferromagnetic phase due to the long-

*Electronic address: aschweig@physics.bu.edu

range interactions. First, we introduce the potential:

$$V(\phi) = \epsilon\phi^2 + u\phi^4 - h\phi, \quad (1)$$

where $\epsilon < 0$, $u > 0$, and $h \neq 0$ is the external magnetic field. For systems of interaction range R , the Ginzburg-Landau-Wilson Hamiltonian is

$$H[\phi] = \int dx \left[\frac{R^2}{2} \left(\frac{d\phi}{dx} \right)^2 + V(\phi(x)) \right]. \quad (2)$$

We assume purely dissipative dynamics, given by the time-dependent Ginzburg-Landau equation,

$$\frac{\partial\phi}{\partial t} = -\frac{\delta H}{\delta\phi} + \eta = R^2 \frac{\partial^2\phi}{\partial x^2} - 2\epsilon\phi - 4u\phi^3 + h + \eta, \quad (3)$$

where $\eta = \eta(x, t)$ is a zero-mean white noise with $\langle \eta(x, t)\eta(x', t') \rangle = 2\beta^{-1}\delta(x - x')\delta(t - t')$, and β is the inverse temperature. The mean-field metastable well vanishes when the applied magnetic field is the spinodal field, $h_{\text{sp}}^2 = 8|\epsilon|^3/27u$. The corresponding mean-field spinodal magnetization is $\phi_{\text{sp}}^2 = |\epsilon|/6u$. These are obtained from setting $dV/d\phi = d^2V/d\phi^2 = 0$. As a matter of convention, we assume that after the quench, the applied magnetic field is positive, hence $h_{\text{sp}} > 0$ and $\phi_{\text{sp}} < 0$.

Near the spinodal, the applied magnetic field after the quench is nearly the spinodal magnetic field, therefore $h_{\text{sp}} - h \ll 1$. It is convenient to introduce $\Delta_h = h_{\text{sp}} - h$, a measure of the depth of the metastable well.

We expand the potential about the spinodal magnetization, ϕ_{sp} , retaining terms up to third order [16, 17]:

$$\begin{aligned} V = & -|\phi_{\text{sp}}| \left(\Delta_h - \frac{3}{8}h_{\text{sp}} \right) + \Delta_h(\phi - \phi_{\text{sp}}) \\ & - \frac{1}{2} \frac{h_{\text{sp}}}{\phi_{\text{sp}}^2} (\phi - \phi_{\text{sp}})^3 + O((\phi - \phi_{\text{sp}})^4). \end{aligned} \quad (4)$$

We will concentrate on nucleation in the neighborhood of the metastable well; the details of the potential for large positive magnetizations will have a negligible effect on nucleation. Within this approximation, the location of the potential minimum is

$$\phi_{\text{min}} = -|\phi_{\text{sp}}| \left[1 + \sqrt{\frac{2\Delta_h}{3h_{\text{sp}}}} \right]. \quad (5)$$

We shift the field, $\psi(x) = \phi(x) + \phi_{\text{min}}$, and drop an overall constant term in the potential. The resulting potential is

$$V(\psi) = \frac{\sqrt{6h_{\text{sp}}\Delta_h}}{2|\phi_{\text{sp}}|} \psi^2 - \frac{1}{2} \frac{h_{\text{sp}}}{\phi_{\text{sp}}^2} \psi^3. \quad (6)$$

This cubic approximation of the potential will be the starting point for our description of transient nucleation. For notational convenience, we introduce the variables

$a = \sqrt{6h_{\text{sp}}\Delta_h}/(2|\phi_{\text{sp}}|) > 0$ and $b = h_{\text{sp}}/(2\phi_{\text{sp}}^2) > 0$, and we rewrite the potential as $V(\psi) = a\psi^2 - b\psi^3$.

Near the mean-field spinodal, the evolution of the field in the neighborhood of the metastable well is given by a Langevin equation,

$$\frac{\partial\psi}{\partial t} = R^2 \frac{\partial^2\psi}{\partial x^2} - 2a\psi + 3b\psi^2 + \eta. \quad (7)$$

We define the fixed points of the dynamics by setting the noise to zero and finding the steady-state configurations:

$$0 = R^2 \frac{d^2\psi}{dx^2} - 2a\psi + 3b\psi^2. \quad (8)$$

Equation (8) has two spatially uniform solutions, the stable fixed point, $\psi_{\text{min}}(x) = 0$, and an unstable fixed point. There exists another non-uniform fixed point, $\psi_{\mathcal{F}}(x)$, corresponding to the profile of the critical droplet in metastable equilibrium [17, 18]. Because the droplet can appear anywhere in the system, we fix the center of the droplet at $x = 0$. A droplet must be symmetric, $\psi_{\mathcal{F}}(x) = \psi_{\mathcal{F}}(-x)$, and cannot exhibit a sharp peak at its center, $\psi'_{\mathcal{F}}(0) = 0$. At large distances, the droplet magnetization approaches the metastable background, $\lim_{x \rightarrow \pm\infty} \psi_{\mathcal{F}}(x) = 0$. Solving Eq. (8), the non-uniform fixed point is

$$\psi_{\mathcal{F}} = \frac{a}{b} \cosh^{-2} \left[x \sqrt{\frac{a}{2R^2}} \right]. \quad (9)$$

This fixed point is unstable: assuming noiseless dynamics, a random perturbation about $\psi_{\mathcal{F}}$ would cause the system to return to its metastable well with probability 1/2. Linear stability analysis about the non-uniform fixed point reveals a single negative eigenvalue, $-5a/2$. The corresponding eigenvector gives the initial direction of growth (or decay) about the fixed point [16, 19, 20]:

$$\psi_{\mathcal{N}} = \cosh^{-3} \left(x \sqrt{\frac{a}{2R^2}} \right). \quad (10)$$

The amplitude of the growth eigenvector is concentrated at its center; a spinodal critical droplet grows by first filling its center [19].

III. CHARACTERIZING RELAXATION TO METASTABLE EQUILIBRIUM

According to our prescription, to find transient droplets we require the out-of-equilibrium probability distribution [20, 21, 22]. For our treatment, we assume that the system is prepared in equilibrium and quenched at $t = 0$, at which point it begins its relaxation. Formally, the time-evolution of the probability density is given by the master equation. We sidestep the formal solution and use a quasi-static mean-field theory. We assume at

a time t since the quench the probability density of configurations can be approximated by

$$P[\psi|t] \approx C \exp \left\{ -\beta \int dx \left[\frac{R^2}{2} \left(\frac{d\psi}{dx} \right)^2 + F_t \right] \right\}, \quad (11)$$

where C is an undetermined constant, and F_t depends on time and is chosen to be consistent with a known slowly varying parameter, an estimate of the mean-field magnetization. At $t = 0$, Eq. (11) should agree with the equilibrium distribution prior to the quench. At long times, we must recover the metastable potential,

$$\lim_{t \rightarrow \infty} F_t = V(\psi) = a\psi^2 - b\psi^3. \quad (12)$$

Since the quench only changes the magnetic field, we assume only those parameters implicitly depending on h are time-varying in F_t . This assumption implies changes in both the location of the metastable minimum and its curvature. We again employ a cubic approximation for F_t : we expect that the quartic term can still be neglected since this approximation will be used when t is close to t_{eq} , when the system is in metastable equilibrium. Consequently,

$$F_t = A_t(\psi - m_t)^2 - b(\psi - m_t)^3, \quad (13)$$

where A_t and m_t are time-varying parameters. To determine m_t , let $M_0 = m_0 - |\phi_{\min}| < 0$ denote the typical (mean-field) magnetization prior to the quench. After the quench, the evolution of the mean-field magnetization can be approximated, $\dot{m}_t = -2am_t + 3bm_t^2$, hence,

$$m_t = \frac{2am_0}{3bm_0 + (2a - 3bm_0) \exp(2at)}. \quad (14)$$

To determine A_t , we first calculate an effective external field consistent with the location of the metastable minimum. Let $\Delta_J(t)$ denote a time-dependent effective magnetic field. Using Eq. (5) to relate the effective field to the minimum at m_t , we find:

$$m_t = -|\phi_{\text{sp}}| \left[1 + \sqrt{\frac{2\Delta_J}{3h_{\text{sp}}}} \right] - \phi_{\min}, \quad (15)$$

The time-dependent effective field is thus:

$$\begin{aligned} \Delta_J(t) &= \frac{3}{2} \frac{h_{\text{sp}} (m_t + \phi_{\min} + |\phi_{\text{sp}}|)^2}{\phi_{\text{sp}}^2} \\ &= \Delta_h + \frac{(6h_{\text{sp}}\Delta_h)^{1/2}}{|\phi_{\text{sp}}|} |m_t| + \frac{3}{2} \frac{h_{\text{sp}}}{\phi_{\text{sp}}^2} m_t^2 \\ &= \Delta_h + 2a |m_t| + 3b m_t^2. \end{aligned} \quad (16)$$

Note that $\Delta_J(t)$ decreases to Δ_h as m_t approaches zero. We use Eq. (6) to relate the effective field to the quadratic coefficient in F_t ; we find $A_t = \frac{\sqrt{6h_{\text{sp}}\Delta_J(t)}}{2|\phi_{\text{sp}}|} = a\sqrt{\Delta_J/\Delta_h}$.

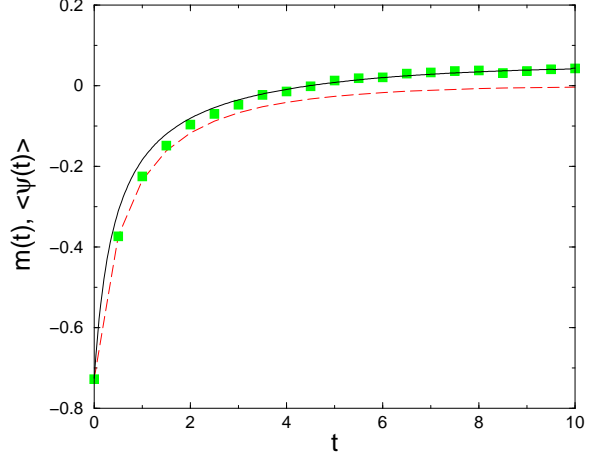


FIG. 1: The mean transient magnetization prior to nucleation (solid line) obtained from the solution of Eq. (3) compared to the average obtained from simulating Eq. (17) in metastable equilibrium (squares). Both curves rise above the metastable minimum (broken line) given by Eq. (14).

Note that A_t decreases in time as the system approaches its metastable equilibrium near the mean-field spinodal.

For a fixed time t , we also define a corresponding Langevin equation:

$$\frac{\partial \psi(x, s)}{\partial s} = R^2 \frac{\partial^2 \psi}{\partial x^2} - F'_t(\psi) + \eta(x, s), \quad (17)$$

where the coordinate s is distinct from the time t since the quench. Once in metastable equilibrium, Eq. (17) samples metastable states from Eq. (11). Figure 1 compares the ensemble-averaged transient magnetization obtained from Eq. (3) to the metastable equilibrium magnetization sampled using Eq. (17) for various t . To estimate the mean metastable magnetization of Eq. (11), we compute the stationary spatial average of Eq. (17),

$$0 = -2A_t [\langle \psi \rangle - m_t] + 3b [\langle \psi^2 \rangle - 2m_t \langle \psi \rangle + m_t^2], \quad (18)$$

which relates the first and second moments. The second moment can be approximated by the second moment of the linear equation obtained by setting $b = 0$:

$$\langle \psi^2 \rangle \approx m_t^2 + \frac{1}{2\beta R (2A_t)^{1/2}}. \quad (19)$$

Equations (18) and (19) yield an estimate of the magnetization, $\langle \psi \rangle$, as a function of the time-dependent parameters, A_t and m_t . This estimate agrees with the simulation averages shown in Fig. 1.

IV. TRANSIENT NUCLEATION

We compute the transient critical droplets, $\psi_C(t)$, by maximizing the probability functional in Eq. (11) con-

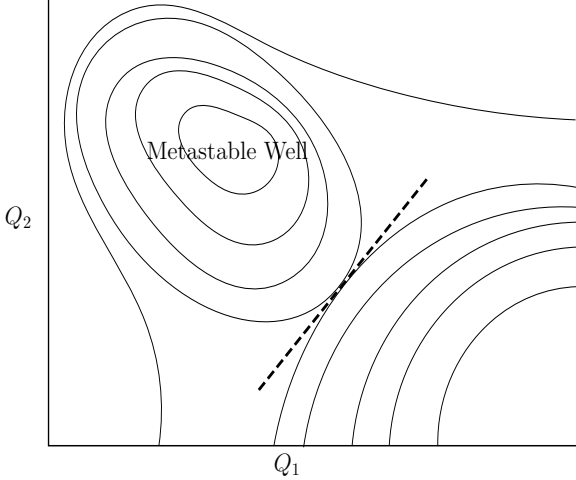


FIG. 2: Equipotential curves for a model system with two dynamical variables, Q_1 and Q_2 . The broken line illustrates the linearization of the metastable well boundary.

strained to the metastable well boundary, \mathfrak{B} :

$$\psi_C(x, t) = \max_{\psi \in \mathfrak{B}} P[\psi | t]. \quad (20)$$

To characterize the boundary, note that the dynamical fixed-point, ψ_F , necessarily lies on the boundary. Furthermore, we assume that our transient critical droplets resemble the dynamical fixed point, ψ_F . We then approximate the metastable well boundary by a hyperplane [15] that is normal to the growth eigenvector, ψ_N , given in Eq. (10). Figure 2 gives a schematic of the approximation for a two-dimensional system. Within this approximation, the set of configurations on the metastable well boundary, $\{\psi_{\mathfrak{B}}\}$, satisfy the equation of a hyperplane:

$$\int dx (\psi_{\mathfrak{B}} - \psi_F) \psi_N = 0. \quad (21)$$

In order to find the object of maximum likelihood that satisfies the constraint, we introduce the Lagrange multiplier λ_t and extremize the functional:

$$\int dx \left[\frac{R^2}{2} \left(\frac{d\psi}{dx} \right)^2 + F_t(\psi) - \lambda_t \psi \psi_N \right]. \quad (22)$$

Centered at zero, the time-dependent critical-droplet profile satisfies:

$$R^2 \frac{d^2 \psi_C}{dx^2} = 2A_t(\psi_C - m_t) - 3b(\psi_C - m_t)^2 - \lambda_t \psi_N, \quad (23)$$

where λ_t is chosen to satisfy the constraint in Eq. (21). For large t , the transient solution reduces to the dynamical fixed point, $\lim_{t \rightarrow \infty} \psi_C = \psi_F$. At earlier times, the equation and constraint can be solved numerically. Because we have assumed the transient critical droplet resembles the fixed point, we expect $\lambda_t \ll 1$. This suggests

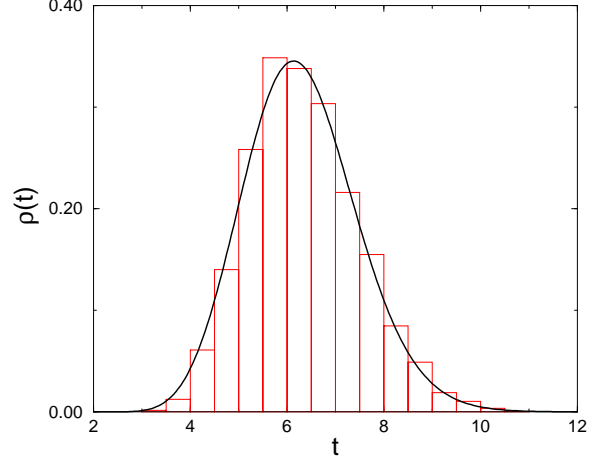


FIG. 3: The theoretical distribution of nucleation times computed from Eq. (29) (solid line) compared to the histogram of nucleation times obtained from direct simulation of Eq. (3).

a solution as a perturbation in λ_t . First, we take $\lambda_t = 0$, and we find the analog to Eq. (9):

$$\psi_C^0(x, t) = m_t + \frac{A_t}{b} \cosh^{-2} \left(x \sqrt{\frac{A_t}{2R^2}} \right). \quad (24)$$

Generally, we have:

$$\psi_C(x, t) = \psi_C^0(x, t) - \lambda_t y(x, t) + O(\lambda_t^2). \quad (25)$$

The resulting differential equation for $y(x)$ is

$$R^2 \frac{d^2 y}{dx^2} = 2 y(x) A_t [1 - 3 \cosh^{-2}(x \sqrt{A_t/2R^2})] + \cosh^{-3}(x \sqrt{A_t/2R^2}). \quad (26)$$

Substituting Eq. (25) into the constraint yields the following equation for the multiplier:

$$\lambda_t = \frac{\int dx (\psi_C^0(x, t) - \psi_F) \psi_N}{\int dx y(x) \psi_N}. \quad (27)$$

With the transient droplet profiles characterized, we finally estimate the time-dependent nucleation rate. Given a time t , we estimate the nucleation rate to be proportional to the probability to realize the corresponding transient critical droplet. In terms of Eqs. (11) and (20),

$$\Gamma(t) = \Gamma_0 P[\psi_C(x, t) | t], \quad (28)$$

where Γ_0 is a prefactor that depends on the details of the system [23]. For the quench considered here, $\Gamma(t)$ is a strictly increasing function of time. The experimentally accessible nucleation time distribution is simply,

$$\rho(t) = \Gamma(t) \exp \left\{ - \int_0^t dt' \Gamma(t') \right\}. \quad (29)$$

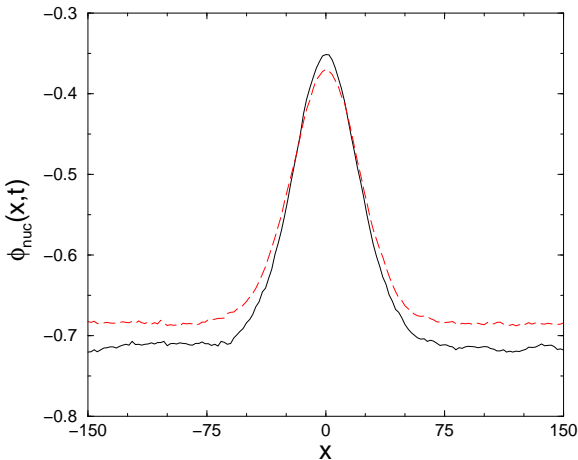


FIG. 4: Ensemble-averaged nucleating-droplet profiles from simulation at $t = 4.5$ (solid line) and $t = 7.5$ (broken line).

V. NUMERICAL CALCULATIONS

We simulated Eq. (3) for a periodic system of length $L = 10^4$ where $\epsilon = -5/9$, $u = 1/4$, $R = 10$, and $\beta = 10$. Prior to the quench, the system is prepared in equilibrium with an external field $h_{initial} = -1.40$ and magnetization $M_0 = -1.442$. After the quench, the applied field is set to $h = 0.430$. The distance to the mean-field spinodal field is $\Delta_h = 0.021$, and the location of the metastable minimum is given by $\phi_{min} = -0.715$. The corresponding parameters in the cubic approximation are $a = 0.195$ and $b = 0.609$.

Throughout the run, the configuration of the system is saved periodically. Once the system has nucleated, we search for the nucleating droplet and nucleation time. We load a saved configuration and find the latest configuration that, upon perturbation, drifts to the stable phase with probability $1/2$. We do not consider runs where multiple droplets appear at the nucleation time. The nucleation times were binned and compared to the theoretical results (see Fig. 3) where the free parameter Γ_0 was chosen to produce the best fit. Ensemble-averaged nucleating droplet profiles for two different times are plotted in Fig. 4. The corresponding theoretical critical droplets obtained from Eq. (25) are plotted in Fig. 5.

VI. SUMMARY AND DISCUSSION

We considered transient nucleation in a long-range one-dimensional ϕ^4 model with dissipative dynamics. We defined the metastable well boundary as the set of configurations balanced between the metastable and stable phases. We estimated the time-dependent likelihood of system configurations. We defined the time-dependent critical droplet as the most likely configuration constrained to lie on the metastable well boundary and com-

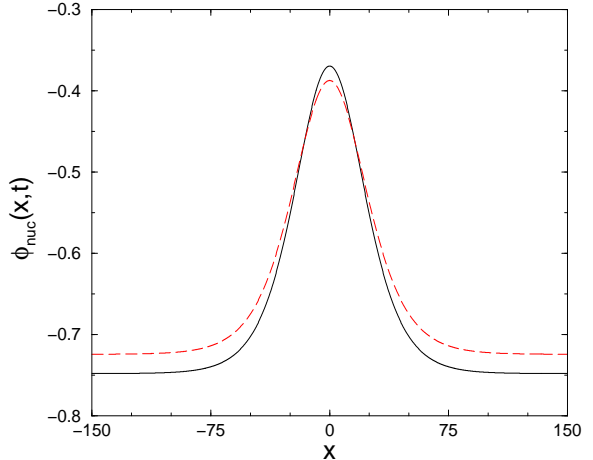


FIG. 5: Theoretical critical-droplet profile from Eq. (25) computed at $t = 4.5$ (solid line) and $t = 7.5$ (broken line).

puted its likelihood at various times. Our results explain the empirically observed non-stationarity of nucleation rates.

The theory is applicable to systems near metastable equilibrium where the system magnetization evolves slowly compared to the relaxation of other dynamical variables, as is the case near a spinodal.

If the time-dependent likelihood, Eq. (11), is Gaussian in the vicinity of the critical-droplet configuration, then the discrepancies between the averaged profiles and the theoretical profiles would vanish. We can ensure the validity of a Gaussian approximation by taking the saddle-point parameter G to be large [17, 18]. However, a large saddle-point parameter suppresses the nucleation rate, $\Gamma \sim L \exp(-\beta G)$, and obscures transience in the nucleating droplets. To preserve the transient-nucleation regime while increasing the saddle-point parameter, the system size L must scale exponentially with G . In the case considered here, the saddle-point parameter is small, $G = Ra^{5/2} = 0.08$. Despite this, the theory provides a qualitative picture of the measured ensemble-averaged profiles. The analysis produces a distribution of nucleation times consistent with the simulation results with a single free parameter.

Our analysis reduces to the earlier work [17, 18] for large t , when the system has relaxed to metastable equilibrium. Qualitatively, we found that early nucleating droplets decay to the background magnetization in the system at the time of nucleation. At early times, the background magnetization is further from the metastable phase magnetization and consequently acts as an anchor: transient droplets must have greater amplitude, which in turn suppresses their rate of formation. Furthermore, it suggests that in comparable experiments, transient effects may result in configurations that are more compact than predicted by the metastable equilibrium analysis.

VII. ACKNOWLEDGMENTS

We thank V. Sood, A. Santos, K. Barros, H. Wang, J. Fiala, and H. Gould for their useful insights and discus-

sions. We also acknowledge the support of DOE grant DE-FG02-95ER14498.

[1] S. R. Stiffler, M. O. Thompson, and P. S. Peercy, “Transient nucleation following pulsed-laser melting of thin silicon films,” *Phys. Rev. B* **43**, 9851 (1991).

[2] H. Kumomi and T. Yonehara, “Transient nucleation and manipulation of nucleation sites in solid-state crystallization of a-Si films,” *J. Appl. Phys.* **75**, 2884 (1994).

[3] Y. X. Zhuang, J. Z. Jiang, Z. G. Lin, M. Mezouar, W. Crichton, and A. Inoue, “Evidence of eutectic crystallization and transient nucleation in $\text{Al}_{89}\text{La}_6\text{Ni}_5$ amorphous alloy,” *Appl. Phys. Lett.* **79**, 743 (2001).

[4] V. Sergan, Y. Reznikov, J. Anderson, P. Watson, J. Ruth, and P. Bos, “Mechanism of relaxation from electric field induced homeotropic to planar texture in cholesteric liquid crystals,” *Mol. Cryst. Liq. Cryst.* **330**, 1339 (1999).

[5] Ya. B. Zeldovich, *Acta Physicochim. URSS* **18**, 1 (1943).

[6] K. F. Kelton, A. L. Greer, and C. V. Thompson, “Transient nucleation in condensed systems,” *J. Chem. Phys.* **79**, 6261 (1983).

[7] V. A. Shneidman, “Transient critical flux in nucleation theory,” *Phys. Rev. A* **44**, 2609 (1991).

[8] B. E. Wyslouzil and G. Wilemski, “Binary nucleation kinetics. III. Transient behavior and time lags,” *J. Chem. Phys.* **105**, 1090 (1996).

[9] I. L. Maksimov, M. Sanada, and K. Nishioka, “Energy barrier effect on transient nucleation kinetics: Nucleation flux and lag-time calculation,” *J. Chem. Phys.* **113**, 3323 (2000).

[10] D. Kashchiev, “Moments of the rate of nonstationary nucleation,” *J. Chem. Phys.* **122**, 114506 (2005).

[11] D. Boyanovsky, R. Holman, D. S. Lee, and J. P. Silva, “A Note on Thermal Activation,” *Nucl. Phys. B* **441**, 595 (1995).

[12] S. Seunarine and D. McKay, “Additive and multiplicative noise driven systems in 1+1 dimensions: Waiting time extraction of nucleation rates,” *Phys. Rev. D* **64**, 105015 (2001).

[13] H. Wang, K. Barros, A. Schweiger, H. Gould, and W. Klein, in preparation.

[14] N. Gulbahce, H. Gould, and W. Klein, “Zeros of the partition function and pseudospinodals in long-range Ising models,” *Phys. Rev. E* **69**, 036119 (2004).

[15] A. Roy, J. M. Rickman, J. D. Gunton, and K. R. Elder, “Simulation study of nucleation in a phase-field model with nonlocal interactions,” *Phys. Rev. E* **57**, 2610 (1998).

[16] M. Büttiker and R. Landauer, “Nucleation theory of overdamped soliton motion,” *Phys. Rev. A* **23**, 1397 (1981).

[17] C. Unger and W. Klein, “Nucleation theory near the classical spinodal,” *Phys. Rev. B* **29**, 2698 (1984).

[18] J. S. Langer, “Theory of the condensation point,” *Ann. Phys.* **41**, 108 (1967).

[19] C. Unger and W. Klein, “Initial-growth modes of nucleation droplets,” *Phys. Rev. B* **31**, 6127 (1985).

[20] J. S. Langer, “Statistical theory of the decay of metastable states,” *Ann. Phys.* **54**, 258 (1969).

[21] K. Binder, “Time-Dependent Ginzburg-Landau Theory of Nonequilibrium Relaxation,” *Phys. Rev. B* **8**, 3423 (1973).

[22] D. Reguera, J. M. Rubí, and A. Pérez-Madrid, “Fokker-Planck equations for nucleation processes revisited,” *Physica A* **259**, 10 (1998).

[23] The prefactors Γ_0 in Eq. (28) and C in Eq. (11) implicitly depend on time. For a sufficiently compact distribution of nucleation times, both Γ_0 and C are effectively constant.